Stability of fluid flow in a Brinkman porous medium – A numerical study*

SHANKAR B. M.
Department of Mathematics, PES Institute of Technology, Bangalore 560 085, India

KUMAR Jai
ISRO Satellite Centre, Bangalore 560 017, India

SHIVAKUMARA I. S.
Department of Mathematics, Bangalore University, Bangalore 560 001, India

NG Chiu-On
Department of Mechanical Engineering, The University of Hong Kong, Pokfulam Road, Hong Kong, China

Abstract: The stability of fluid flow in a horizontal layer of Brinkman porous medium with fluid viscosity different from effective viscosity is investigated. A modified Orr-Sommerfeld equation is derived and solved numerically using Chebyshev collocation method. The critical Reynolds number Re_c, the critical wave number α_c and the critical wave speed c_c are computed for various values of porous parameter and ratio of viscosities. Based on these parameters, the stability characteristics of the system are discussed in detail. Streamlines are presented for selected values of parameters at their critical state.

Keywords: Brinkman model, Chebyshev collocation method, hydrodynamic stability, modified Orr-Sommerfeld equation.

1. Introduction

The stability of fluid flows in a horizontal channel has been studied extensively and the copious literature available on this topic has been well documented in the book by Drazin and Reid[1]. The interesting finding is that the Poiseuille flow in a horizontal channel becomes unstable to infinitesimal disturbances when the Reynolds number exceeds the critical value 5772. The corresponding problem in a porous medium has attracted limited attention of researchers despite its wide range of applications in geothermal operations, petroleum industries, thermal insulation and in the design of solid-matrix heat exchangers to mention a few. In particular, with

* Corresponding author: NG Chiu-On, Email: cong@hku.hk

the advent of hyperporous materials there has been a substantial increase in interest in the study of stability of fluid flows through porous media in recent years as it throws light relating to the onset of macroscopic turbulence in porous media (Lage et al.[2]).

The hydrodynamic stability of flow of an incompressible fluid through a plane- parallel channel or circular duct filled with a saturated sparsely packed porous medium has been discussed on the basis of an analogy with a magneto-hydrodynamic problem by Nield[3]. By employing the Brinkman model with fluid viscosity same as effective viscosity, Makinde[4] investigated the temporal development of small disturbances in a pressure-driven fluid flow through a channel filled with a saturated porous medium. The critical stability parameters were obtained for a wide range of the porous medium shape factor parameter.

The porous materials used in many technological applications of practical importance possess high permeability values. For example, permeabilities of compressed foams as high as $8\times10^{-6}\,\mathrm{m}^2$ and for a 1 mm thick foam layer the equivalent Darcy number is equal to 8 (see Nield et al.[5] and references therein). Moreover, for such a high porosity porous medium, Givler and Altobelli[6] determined experimentally that $\mu_e = 7.5^{+3.4}_{-2.4}\mu$, where μ_e is the effective viscosity or the Brinkman viscosity and μ is the fluid viscosity. Therefore, it is imperative to consider the ratio of these two viscosities different from unity in analyzing the problem. In the present study, the ratio of these two viscosities has been considered as a separate parameter and its influence on the stability characteristics of the system is discussed. The resulting eigenvalue problem is solved numerically using Chebyshev collocation method.

2. Mathematical Formulation

We consider the flow of an incompressible viscous fluid through a layer of sparsely packed porous medium of thickness $2h$, which is driven by an external pressure gradient. The bounding surfaces of the porous layer are considered to be rigid and a Cartesian coordinate system is chosen such that the origin is at the middle of the porous layer as shown in Fig. 1.

The governing equations are:

$$\nabla\cdot\vec{q} = 0 \tag{1}$$

$$\rho\left[\frac{1}{\varepsilon}\frac{\partial\vec{q}}{\partial t} + \frac{1}{\varepsilon^2}\left(\vec{q}\cdot\nabla\right)\vec{q}\right] = -\nabla p + \mu_e\nabla^2\vec{q} - \frac{\mu}{k}\vec{q} \tag{2}$$

where $\vec{q} = (u, 0, w)$ the velocity vector, ρ the fluid density, p the pressure, μ_e the effective viscosity, μ the viscosity of the fluid, k the permeability and ε the porosity of the porous medium. Let us render the above equations dimensionless using the quantities

$$\vec{q}^* = \frac{\vec{q}}{\bar{U}_B},\ \nabla^* = h\nabla,\ t^* = \frac{t}{h\varepsilon / \bar{U}_B},\ p^* = \frac{p}{\rho \bar{U}_B^2} \tag{3}$$

where $\bar{U}_B$ is the average base velocity. Equation (3) is substituted in Eqs. (1) and (2) to obtain (after discarding the asterisks for simplicity)

$$\nabla \cdot \vec{q} = 0 \tag{4}$$

$$\frac{\partial \vec{q}}{\partial t} + (\vec{q} \cdot \nabla)\vec{q} = -\varepsilon^2 \nabla p + \frac{\Lambda}{Re}\nabla^2 \vec{q} - \frac{\sigma_p^2}{Re}\vec{q}. \tag{5}$$

Here, $Re = \bar{U}_B\, d / \nu$ is the Reynolds number, where ν $(= \mu / \rho)$ is the kinematic viscosity, $\Lambda = \varepsilon^2 \mu_e / \mu$ is the ratio of effective viscosity to the viscosity of the fluid and $\sigma_p = \varepsilon h / \sqrt{k}$ is the porous parameter.

2.1 Base flow

The base flow is steady, laminar and fully developed, that is, it is a function of z only. With these assumptions, Eq. (5) reduces to

$$Re\, \varepsilon^2 \frac{dp_b}{dx} = \Lambda \frac{d^2 U_B}{dz^2} - \sigma_p^2 U_B \tag{6}$$

The associated boundary conditions are

$$U_B = 0 \quad \text{at } z = \pm 1 \tag{7}$$

Solving Eq. (6) using the above boundary conditions, we get

$$U_B = \frac{\cosh\left(\frac{\sigma_p}{\sqrt{\Lambda}}\right) - \cosh\left(\frac{\sigma_p}{\sqrt{\Lambda}}\, z\right)}{\cosh\left(\frac{\sigma_p}{\sqrt{\Lambda}}\right) - 1}. \tag{8}$$

The above basic velocity profile coincides with the Hartmann flow if $\sigma_p / \sqrt{\Lambda}$ is identified with the Hartmann number (Lock[7], Takashima[8]).

2.2 Linear Stability Analysis

To study the linear stability analysis, we superimpose an infinitesimal disturbance on the base flow in the form

$$\vec{q} = U_B(z)\hat{i} + \vec{q}', \quad p = p_b(z) + p'. \tag{9}$$

Substituting Eq. (9) into Eqs. (4) and (5), linearizing and restricting our attention to two-dimensional disturbances, we obtain (after discarding the asterisks for simplicity)

$$\frac{\partial u}{\partial x} + \frac{\partial w}{\partial z} = 0 \tag{10}$$

$$\frac{\partial u}{\partial t} + U_B \frac{\partial u}{\partial x} + DU_B w = -\frac{\partial p}{\partial x} + \frac{\Lambda}{Re}\nabla^2 u - \frac{\sigma_p^2}{Re}u \tag{11}$$

$$\frac{\partial w}{\partial t} + U_B \frac{\partial w}{\partial x} = -\frac{\partial p}{\partial z} + \frac{\Lambda}{Re}\nabla^2 w - \frac{\sigma_p^2}{Re}w \tag{12}$$

To discuss the stability of the system, we use the normal mode solution of the form

$$\{u, w\}(x, z, t) = \{u, w\}(z)e^{i\alpha(x-ct)} \tag{13}$$

where $c = c_r + ic_i$ is the wave speed, c_r is the phase velocity and c_i is the growth rate and α is the horizontal wave number which is real and positive. If $c_i > 0$, then the system is unstable and if $c_i < 0$, then the system is stable. Equations (10) to (12), using Eq. (13) and after simplification, respectively become

$$i\alpha u + Dw = 0 \tag{14}$$

$$\left[\Lambda\left(D^2 - \alpha^2\right) - i\alpha Re\left(U_B - c\right)\right]u = i\alpha Re\, p + ReDU_B w + \sigma_p^2 u \tag{15}$$

$$\left[\Lambda\left(D^2 - \alpha^2\right) - i\alpha Re\left(U_B - c\right)\right]w = Re\, Dp + \sigma_p^2 w \tag{16}$$

where $D = d/dz$ is the differential operator. First, the pressure p is eliminated from the momentum equations by operating D on Eq. (15), multiplying Eq. (16) by $i\alpha$ and subtracting the resulting equations and then a stream function $\psi(x, z, t)$ is introduced through

$$u = \frac{\partial \psi}{\partial z}, w = -\frac{\partial \psi}{\partial x} \tag{17}$$

to obtain an equation for $\psi(x, z, t)$ in the form

$$\Lambda(D^2 - \alpha^2)^2\psi - \sigma_p^2(D^2 - \alpha^2)\psi = i\alpha Re\left[(U_B - c)(D^2 - \alpha^2)\psi - D^2U_B\psi\right]. \tag{18}$$

Equation (18) is the required stability equation which is the modified form of Orr-Sommerfeld equation and reduces to the one obtained for an ordinary viscous fluid if $\sigma_p = 0$ and $\Lambda = 1$.

The boundaries are rigid and the appropriate boundary conditions are:

$$\psi = D\psi = 0 \quad \text{at } z = \pm 1. \tag{19}$$

3. Method of Solution

Equation (18) together with the boundary conditions (19) constitutes an eigenvalue problem which has to be solved numerically. The resulting eigenvalue problem is solved using Chebyshev collocation method.

The k^{th} order Chebyshev polynomial is given by

$$T_k(z) = \cos k\theta, \ \theta = \cos^{-1} z. \tag{20}$$

The Chebyshev collocation points are given by

$$z_j = \cos\left(\frac{\pi j}{N}\right), \ j = 0(1)N. \tag{21}$$

Here, the lower and upper wall boundaries correspond to $j = 0$ and N, respectively. The field variable ψ can be approximated in terms of Chebyshev variable as follows

$$\psi(z) = \sum_{j=0}^{N} T_n(z_j)\psi_j. \tag{22}$$

The governing equations (18) and (19) are discretized in terms of Chebyshev variable z to get

$$\begin{aligned} &\Lambda\left(\sum_{k=0}^{N} C_{jk}\psi_k + \alpha^4\psi_j - 2\alpha^2\sum_{k=0}^{N} B_{jk}\psi_k\right) - \sigma_p^2\left(\sum_{k=0}^{N} B_{jk}\psi_k - \alpha^2\psi_j\right) = \\ &\qquad i\alpha Re\left[(U_B - c)\left(\sum_{k=0}^{N} B_{jk}\psi_k - \alpha^2\psi_j\right) - D^2U_B\psi_j\right] = 0, \ \ j = 1(1)N-1 \end{aligned} \tag{23}$$

$$\psi_0 = \psi_N = 0 \tag{24}$$

$$\sum_{k=0}^{N} A_{jk}\psi_k = 0, \quad j = 0 \ \& \ N \tag{25}$$

where

$$A_{jk}=\begin{cases}\dfrac{c_j(-1)^{k+j}}{c_k(z_j-z_k)} & j\neq k\\ \dfrac{z_j}{2(1-z_j^2)} & 1\le j=k\le N-1\\ \dfrac{2N^2+1}{6} & j=k=0\\ -\dfrac{2N^2+1}{6} & j=k=N\end{cases} \tag{26}$$

$$B_{jk}=A_{jm}\cdot A_{mk}\ \&\ C_{jk}=B_{jm}\cdot B_{mk}\,. \tag{27}$$

with

$$c_j=\begin{cases}2 & j=0,N\\ 1 & 1\le j\le N-1.\end{cases}\,.$$

The above equations form the following system of linear algebraic equations

$$AX=cBX \tag{28}$$

where A and B are the complex matrices, c is the eigenvalue and X is the eigenvector. To solve the above generalized eigenvalue problem, the DGVLCG of IMSL library[9] is employed. The routine is based on the QZ algorithm due to Molar and Stewart[10]. The first step of this algorithm is to simultaneously reduce A to upper Heisenberg form and B to upper triangular form. Then, orthogonal transformations are used to reduce A to quasi-upper-triangular form while keeping B upper triangular. The eigenvalues for the reduced problem are then computed as follows.

For fixed values of Λ, σ_p and Re, the values of c which ensure a non-trivial solution of Eq. (28) are obtained as the eigenvalues of the matrix $B^{-1}A$. From $2N$ eigenvalues $c(1)$, $c(2)$, $\cdots$, $c(2N)$, the one having the largest imaginary part of ($c(p)$, say) is selected. In order to obtain the neutral stability curve, the value of Re for which the imaginary part of $c(p)$ vanishes is sought. Let this value of Re be Re_q. The lowest point of Re_q as a function of α gives the critical Reynolds number Re_c and the critical wave number α_c. The real part of $c(p)$ corresponding to Re_c and α_c gives the critical wave speed c_c. This procedure is repeated for various values of Λ and σ_p.

4. Results and Discussion

The stability of fluid flow in a horizontal layer of Brinkman porous medium with fluid viscosity different from effective viscosity is investigated using Chebyshev collocation method. To know the accuracy of the method employed, it is instructive to look at the wave speed as a function of order of Chebyshev polynomials. Table 1 illustrates this aspect for different orders of Chebyshev polynomials ranging from 1 to 100. It is observed that four digit point accuracy was achieved by retaining 50 terms in Eq. (22). As the number of terms increases in Eq. (22), the results found to remain consistent and the accuracy improved up to 7 digits and 10 digits for N = 80 and N = 100, respectively. In the present study, the results are presented by taking N = 80. The critical stability parameters computed for various values of porous parameter σ_p are tabulated in Tables 2 and 3 for two values of ratio of viscosities $\Lambda = 1$ and 2, respectively. The results for σ_p = 0 in Table 1 correspond to the stability of classical plane-Poiseuille flow. For this case, it is seen that Re_c = 5772.955239, α_c =1.02 and c_c = 0.264872176035885 which are in excellent agreement with those reported in the literature[1].

The neutral stability curves are displayed in Fig. 2 for different values of σ_p and for two values of $\Lambda = 1$ and 2. The portion below each neutral curve corresponds to stable region and the region above corresponds to instability. It may be noted that, increase in σ_p and Λ leads to an increase in the critical Reynolds number and thus they have stabilizing effect on the fluid flow. The lowest curve in the figure corresponds to the classical plane-Poiseuille flow case.

Figures 3(a), (b) and (c) respectively show the variation of critical Reynolds number Re_c, critical wave number α_c and the critical wave speed c_c as a function of porous parameter σ_p for two values of ratio of viscosities $\Lambda = 1$ and 2. It is observed that increase in the porous parameter is to increase Re_c and thus it has stabilizing effect on the fluid flow due to decrease in the permeability of the porous medium. Besides, increase in the ratio of viscosities has a stabilizing effect on the fluid flow due to increase in the viscous diffusion. The critical wave number exhibits a decreasing trend initially with σ_p but increases with further increase in the value of the same. Although initially the critical wave number for $\Lambda = 2$ are higher than those of $\Lambda = 1$, the trend gets reversed with increasing values of σ_p. The critical wave speed decreases

with increasing porous parameter and remains constant as σ_p increases. Moreover, the critical wave speed decreases with increasing Λ and becomes independent of ratio of viscosities with increasing porous parameter.

The variation in the growth rate of the most unstable mode against the wave number for different values of porous parameter with $\Lambda = 1$ and for different values of ratio of viscosities with $\sigma_p = 3$ is illustrated in Figs. 4(a) and (b), respectively. It is observed that increasing the value of porous parameter is to suppress the disturbances and thus its effect is to eliminate the growth of small disturbances in the flow. Although similar is the effect with increasing the value of ratio of viscosities at lower and higher wave number regions, an opposite kind of behavior could be seen at intermediate values of wave number.

Figures 5 and 6 show the streamlines for different values of σ_p for $\Lambda = 1$ and 2, respectively at their critical state. It is observed that there is a significant variation in the streamlines pattern with varying σ_p and Λ. As the value of σ_p increases from 0 to 5, the strength of secondary flow decreases but flow profile remains same. In this regime, convective cells are unicellular and cells are spread throughout the domain. Figure 5(d) indicates that for σ_p = 20 the secondary flow becomes double-cellular but flow is only near to walls of the channel. As value of σ_p increases further the flow strength again increases and convective cells becomes unicellular. The streamlines pattern illustrated in Fig. 6 for $\Lambda = 2$ exhibits a similar behavior.

5. Conclusions

The temporal development of infinitesimal disturbances in a horizontal layer of Brinkman porous medium with fluid viscosity different from effective viscosity is studied numerically using Chebyshev collocation method. It is found that the ratio of viscosities has a profound effect on the stability of the system and increase in its value is to stabilize the fluid flow. Besides increase in the value of porous parameter has stabilizing effect on the fluid flow. The secondary flow for $\Lambda = 1$ and 2 is spread throughout the domain at lower values of σ_p but confined in the middle of the domain at higher values. Secondary flow pattern remains same for both values of viscosity ratios considered here.

Acknowledgements The author B.M.S wishes to thank the Head of the Department of Science and Humanities, Principal and the Management of the college for encouragement

References

[1] Drazin P. G. and Reid W. H. **Hydrodynamic Stability**[M]. Cambridge, UK: Cambridge University Press, 2004.

[2] Lage J. L., De Lemos M. J. S. and Nield D. A. Modeling turbulence in porous media, in: Ingham D. B. and Pop I. (Eds.), **Transport Phenomena in Porous Media II**[M]. Oxford, UK: Elsevier Science, 2002, 198–230.

[3] Nield D. A. The stability of flow in a channel or duct occupied by a porous medium[J]. **International Journal of Heat and Mass Transfer**, 2003, 46: 4351–4354.

[4] Makinde O. D. On the Chebyshev collocation spectral approach to stability of fluid flow in a porous medium[J]. **International Journal for Numerical Methods in Fluids**, 2009, 59: 791–799.

[5] Nield D. A., Junqueira S. L. M. and Lage J. L. Forced convection in a fluid saturated porous medium channel with isothermal or isoflux boundaries[C]. **Proceedings of the First International Conference on Porous Media and Their Applications in Science, Engineering and Industry**. Kona, Hawaii, USA, 1996, 51–70.

[6] Givler R. C. and Altobelli S. A. A determination of the effective viscosity for the Brinkman-Forchheimer flow model[J]. **Journal of Fluid Mechanics**, 1994, 258: 355–370.

[7] Lock R. C. The stability of the flow of an electrically conducting fluid between parallel planes under a transverse magnetic field[J]. **Proceeding of the Royal Society A**, 1955, 233: 105–125.

[8] Takashima M. The stability of the modified plane Poiseuille flow in the presence of a transverse magnetic field[J]. **Fluid Dynamics Research**, 1996, 17: 293–310.

[9] IMSL, International Mathematical and Statistical Library, (1982).

[10] Molar C. B. and Stewart G. W. An algorithm for generalized matrix eigenvalue problems[J]. **SIAM Journal of Numerical Analysis**, 1973, 10(2): 241–256.

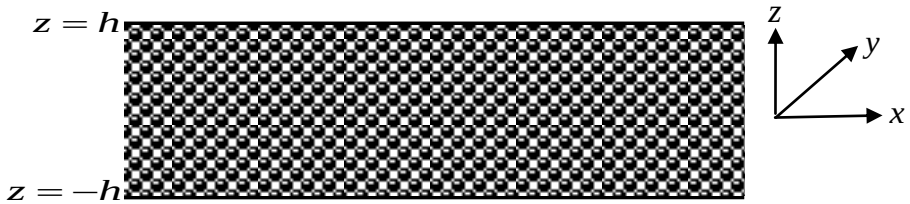

Fig. 1 Physical configuration

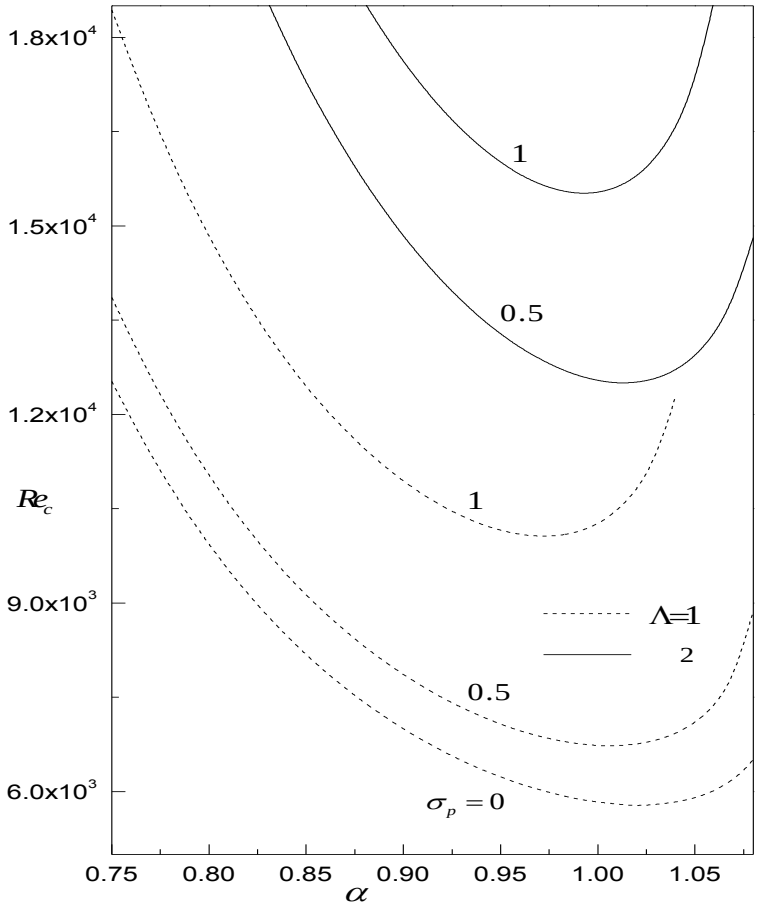

Fig. 2 Neutral curves for different values of σ_p and Λ

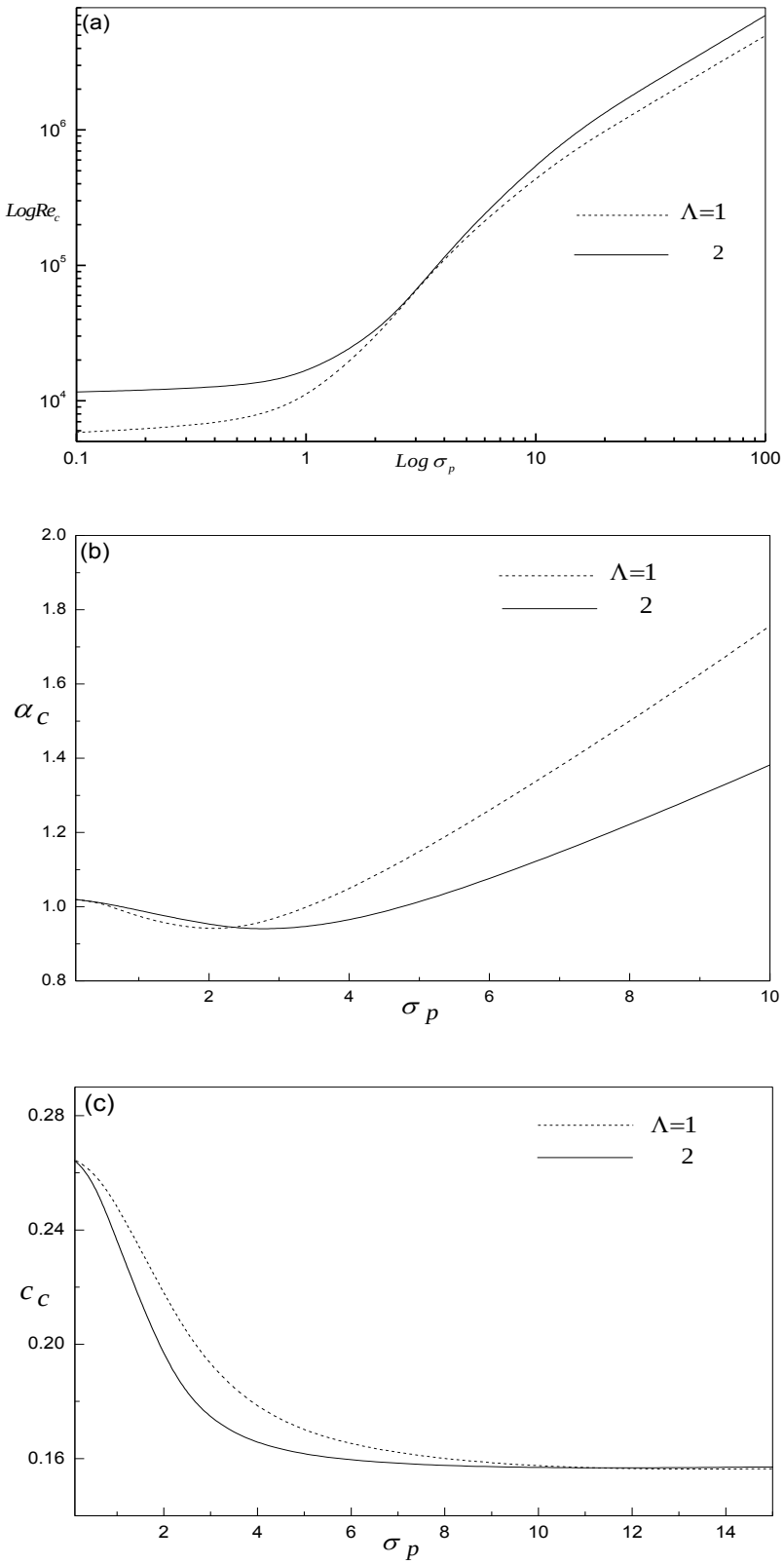

Fig. 3 Variation of (a) Re_c, (b) α_c and (c) c_c with σ_p for two values of Λ

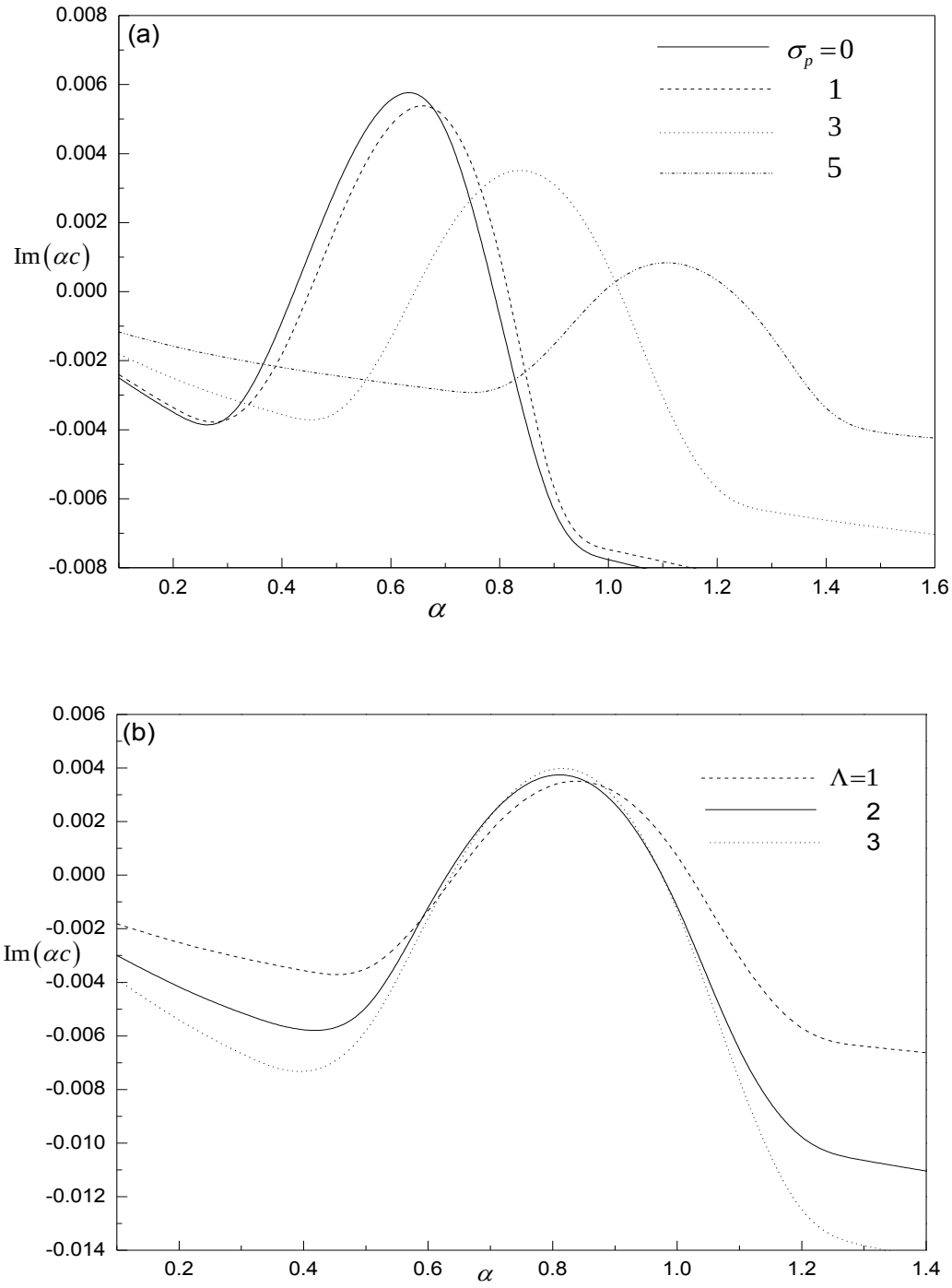

Fig. 4 Variation of growth rate $\mathrm{Im}(\alpha c)$ against α for different values of (a) σ_p with $\Lambda = 1$ and (b) Λ with σ_p =3 when $Re = 2\times10^5$

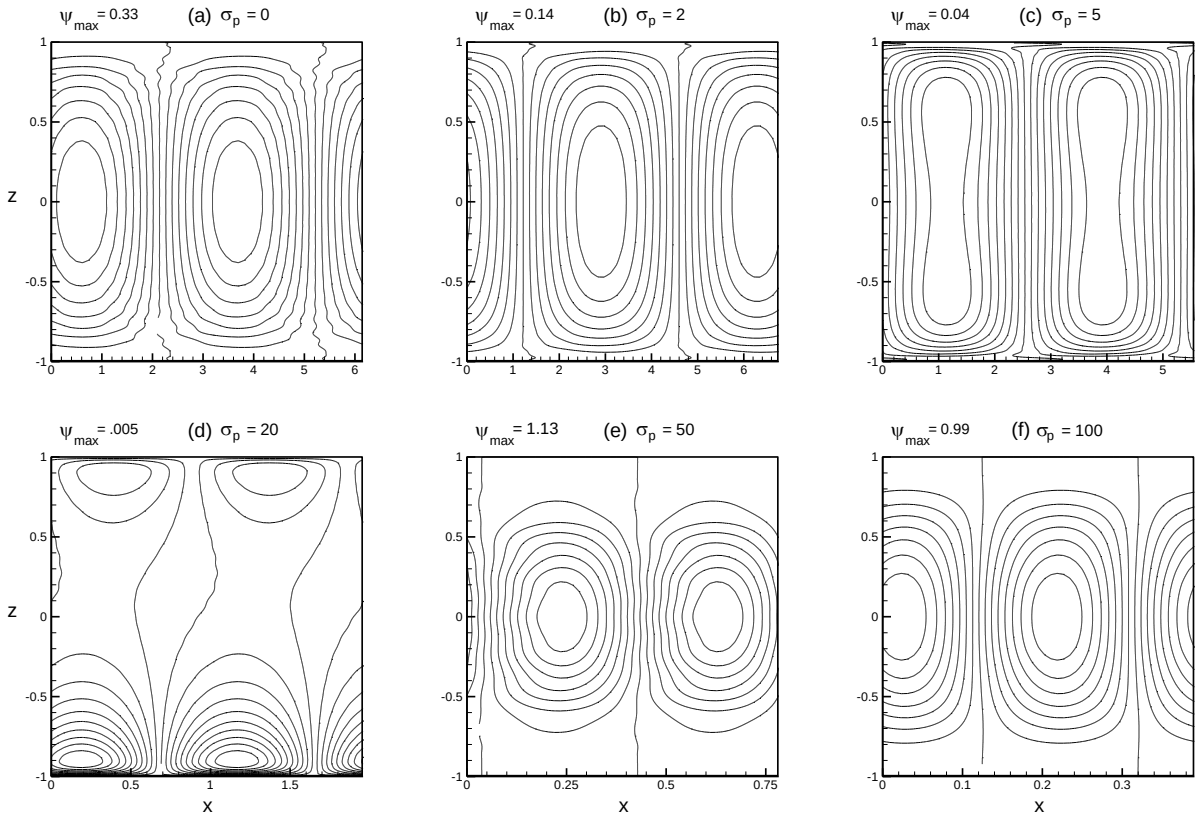

Fig. 5 Streamlines for $\Lambda = 1$

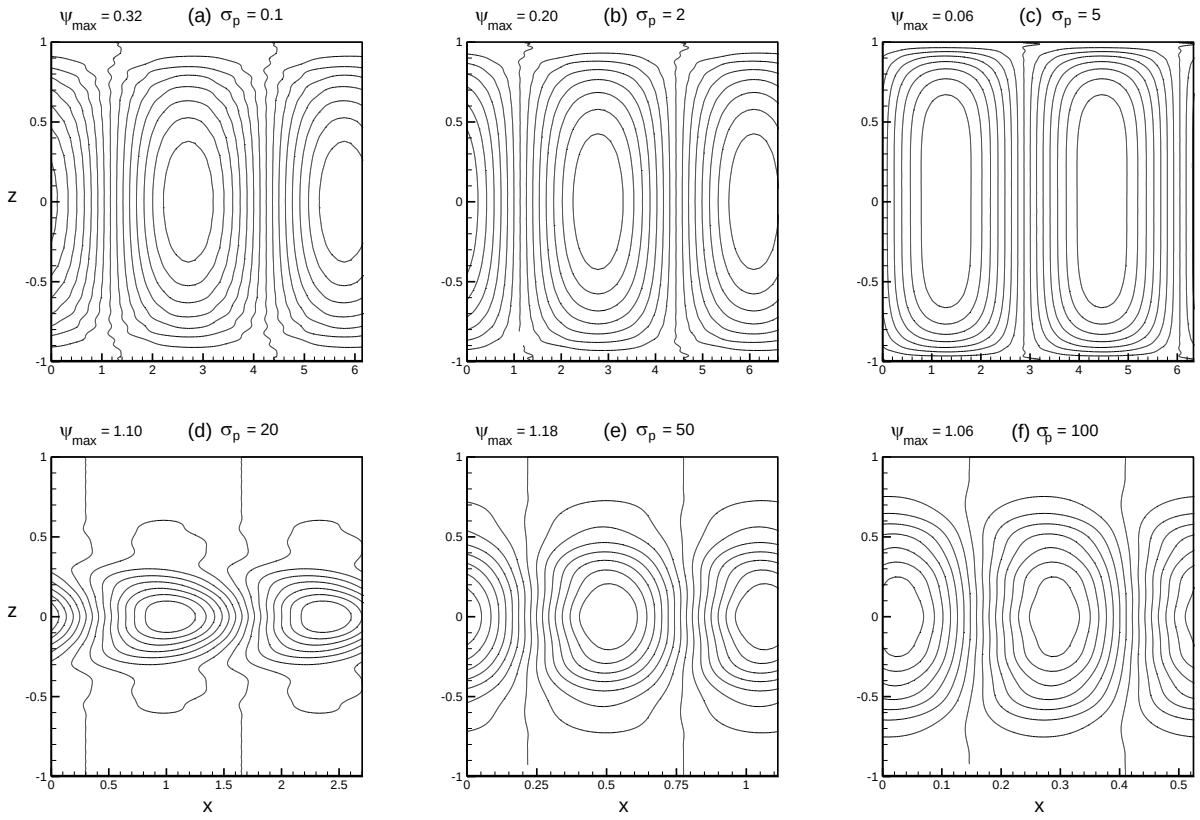

Fig. 6 Streamlines for $\Lambda = 2$

N	c
5	0.693518107893652 - 0.000083844138659i
10	0.402924970355927 +0.000003543182553i
15	0.252788317613093 +0.001402916654061i
20	0.182901607284347 +0.002557008891944i
25	0.910087603387166 - 0.003680141263285i
30	0.936838760905464 - 0.004555530852476i
35	0.953239931934621 - 0.005421331881951i
40	0.964045306550104 - 0.006571837595488i
45	0.961511990916474 - 0.007811518881257i
50	0.961907403228478 - 0.007838410021033i
55	0.961160636215249 - 0.007837875616178i
60	0.991127232587008 - 0.007812092027005i
65	0.991126785122664 - 0.007812091212242i
70	0.991124064507403 - 0.007812085576797i
75	0.991124619603898 - 0.007812085369762i
80	0.991124645294663 - 0.007812085220502i
85	0.991124632576554 - 0.007812085278582i
90	0.991124632014134 - 0.007812085210679i
95	0.991124632233021 - 0.007812085246101i
100	0.991124632209442 - 0.007812085253386i

Table 1: Order of polynomial independence for $\sigma_p = 0.5$, $Re = 20000$, $\alpha = 1$ and $\Lambda = 1$

σ_p	Re_c	α_c	c_c
0.0	5772.955239	1.02	0.264872176035885
0.1	5823.724407	1.02	0.264608547359021
0.5	6729.754766	1.01	0.257302683215492
1.0	10058.784500	0.97	0.236348982126750
2.0	28760.892790	0.93	0.193657950030372
3.0	65679.747074	0.96	0.170892426624650
5.0	167022.968293	1.13	0.158919307085916
10.0	443074.155792	1.74	0.156348745969234
15.0	719431.119028	2.45	0.157129203516859
20.0	983227.239208	3.21	0.157675732484102
30.0	1481009.215883	4.81	0.157720964450717
50.0	2500140.143218	8.03	0.157720974641616
100.0	4969163.123916	16.10	0.157720987503782

Table 2: Values of Re_c, α_c and c_c for different values of σ_p when $\Lambda = 1$

σ_p	Re_c	α_c	c_c
0.1	11611.630425	1.02	0.264740362734358
0.5	12496.046066	1.01	0.260452559673983
1.0	15513.694555	0.99	0.249116441034995
2.0	31057.685083	0.95	0.217397368338407
3.0	64702.301025	0.93	0.189782908769432
5.0	181131.896972	0.99	0.164717429222772
10.0	555919.589576	1.37	0.155972156146598
15.0	954466.394318	1.82	0.156442820186782
20.0	1345948.408540	2.32	0.157000299420360
30.0	2069885.987405	3.42	0.157078870409787
50.0	3474185.249230	5.63	0.157079351092361
100.0	6999130.237221	11.94	0.157079448297211

Table 3: Values of Re_c, α_c and c_c for different values of σ_p when $\Lambda = 2$